Supporting Information (SI)

Antibody fluorescein-doped silica nanobioconjugates for ultrasensitive detection of prostate-specific antigen

Tumelo Msutu,[a] Omotayo Adeniyi,[a] and Philani Mashazi[a,b,*]

[a]Department of Chemistry, Rhodes University, P.O. Box 94, Makhanda, 6140, South Africa.

[b]Institute for Nanotechnology Innovation, Rhodes University, P.O. Box 94, Makhanda, 6140, South Africa.

*Corresponding Author: p.mashazi@ru.ac.za

1 Experimental

1.1 Materials and reagents

Fluorescien-5-isothiocyanate Isomer 1 (FITC, 90%), (3-aminopropyl)triethoxysilane (APTES, 98%), tetraethyl orthosilicate (TEOS, 99.9%), 4-carboxyphenylboronic acid, sodium chloride (NaCl), N-hydroxysuccinimide (NHS), sodium hydroxide (NaOH), 4-(1,1,3,3-tetramethylbutyl)-phenyl polyethylene glycol (Triton X-100), disodium hydrogen phosphate (Na_2HPO_4), sodium dihydrogen phosphate (NaH_2PO_4), 1-ethyl-3-(3-dimethylaminopropyl) carbodiimide hydrochloride (EDC), Bovine serum albumin (BSA), and deuterated methanol (d_4-MeOH) were purchased from Sigma-Aldrich (USA). Sodium hydrogen carbonate ($NaHCO_3$), sodium carbonate anhydrous (Na_2CO_3), absolute ethanol (98.6%, w/v), and D-glucose were purchased from SAARChem (South Africa). Deuterated dimethyl sulfoxide (d_6-DMSO) was purchased from Merck (South Africa). Cyclohexane (99.5%) was purchased from Merck

(Germany). 1-Hexanol was purchased from B&M Scientific (South Africa). Ammonium hydroxide (NH_4OH, 25% wt) was purchased from Minema Chemicals (South Africa).

Bradford reagent (for Bradford assay) was purchased from Bio-rad Laboratory Ltd (USA). Ultrapure water with a resistivity of 18 MΩ.cm (at 25°C) was obtained from a Milli-Q Water Purification System (Millipore Corp. Bedford, MA, USA) and was used for the preparations of aqueous solutions throughout the experiments. Coupling buffer used, phosphate buffer solution (PBS, pH 7.4, 10 mM) was prepared using 0.28 g sodium chloride, 0.86 g disodium hydrogen phosphate (Na_2HPO_4), 0.72 g sodium dihydrogen orthophosphate (NaH_2PO_4) in 500 mL of ultrapure millipore water. Sodium carbonate buffer (pH 9.6, 10 mM) was prepared using 0.17g sodium bicarbonate ($NaHCO_3$) and 0.21g sodium carbonate (Na_2CO_3) in 200 mL of ultrapure millipore water. All reagents in this study were of analytical grade and used as received from the supplier. FITC-APTES **(3)** and TES-PBA **(5)** were successful synthesized and confirmed using FTIR spectra in **Figure S1** and **Figure S2**, respectively.

1.2 Equipment

Fourier transform infrared spectroscopy (FTIR) analysis was conducted using a Perkin-Elmer Universal ART sampling accessory spectrum 100 FTIR spectrophotometer. UV-vis absorption measurements were recorded using the Shimadzu UV 2550 spectrometer. The fluorescence spectra were recorded using a Spectramax Multitude spectrofluorometer and Synergy MX microplate reader. Zeta potential was obtained with dynamic light scattering (DLS) Malvern Zetasizer Nano series, Nano ZS90 series S equipped with a 633nm He/Ne laser. Transmission

electron microscope (TEM) images were obtained using a Zeiss Libra 120 TEM operating at 80 kV accelerating voltage. For the TEM measurements, nanoparticles were dissolved in a suitable solvent, dropping them onto a carbon-coated copper grid, and allowing them to dry at room temperature before measurements. Energy dispersive X-ray spectroscopy (EDS) elemental mapping was collected in a high vacuum on a Tescan Vega 2 Scanning Electron Microscopy with a W-filament and on an Oxford INCA Penta-FET-X3 Si(Li) detector, at 20 kV. A Black Nuc 96-well maxisorp microplate purchased from Sigma Aldrich were used to fabricate immunosensors and measure the fluorescence emission spectra for the detection studies.

1.3 Methods

1.3.1 Synthesis of fluorescein-isothiocyanito-3-propyltriethoxysilane (FITC-APTES, **3**), **Scheme S1**

The fluorescent silica precursor (FITC-APTES, **3**) was prepared following a reported method with some modifications.[1,2] Briefly, FITC (**1**, 5.30 mg, 13.5 μmol.L^{-1}) was dissolved in 2.0 mL dry ethanol and stirred at room temperature for 30 min. APTES (**2**, 60 μL, 257 μmol.L^{-1}) was added dropwise into the FITC ethanol solution. The reaction was followed using thin layer chromatography until the reagents have reacted. The colour of the mixture turned from bright yellow to a darker orange. The mixture was allowed to react overnight at room temperature in darkness (to prevent photobleaching). Ethanol was evaporated and the product dried in a desiccator overnight to obtain the organosilane precursor, FITC-APTES **(3)** as an orange-yellowish crystal powder. Yield: 80.1%.

FTIR [(ATR), τ_{max}/cm^{-1}]: 3175 (NH), 1570 (N=C=S), 1103 (O-Si-O), 1054 (Si-O-C), 913 (Si-C). UV-vis [λ (nm) log (ε)]: 492 (3.8).

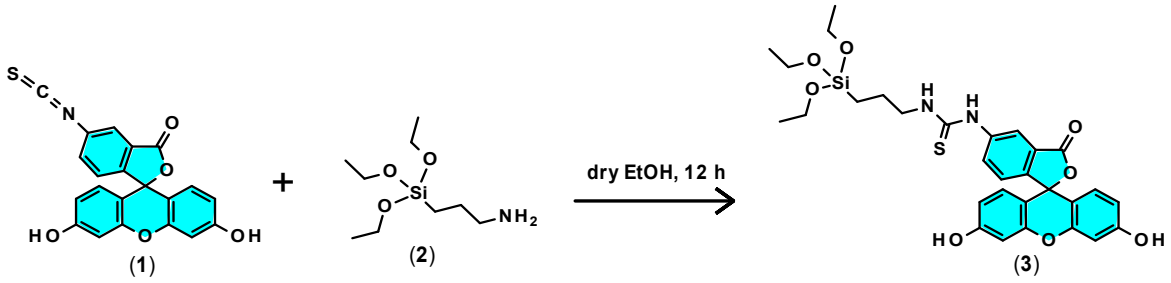

Scheme S1: Synthesis of fluorescein-isothiocynaito-3-propyltriethoxysilane (FITC-APTES, **3**).

1.3.2 Synthesis of triethoxysilanepropyl-3-amidophenylboronic acid (TES-prAmPBA, **5**), **Scheme S2**

4-Carboxyphenylboronic acid (**4**, 166 mg, 1.0 mmol) was added to the solution of EDC (31.0 mg, 0.20 mmol) and NHS (57.5 mg, 0.50 mmol) in dry ethanol (5.0 mL) and stirred for 15 min. APTES (**2**, 0.5 mL, 2.0 mmol) was added dropwise into the solution. The reaction was followed using the thin layer chromatography until the reagents completely reacted. The solution mixture was stirred further for overnight at room temperature until TES-PBA (**5**) resulted, separated, washed with ethanol, and oven dried at 60°C. The product was obtained as a white precipitate. Yield: 66 %.

FTIR [(ATR), τ_{max}/cm^{-1}]: 3228 (OH), 3265 (NH), 1643 (C=O), 1260 (B-O), and 1063 (O-Si-O).

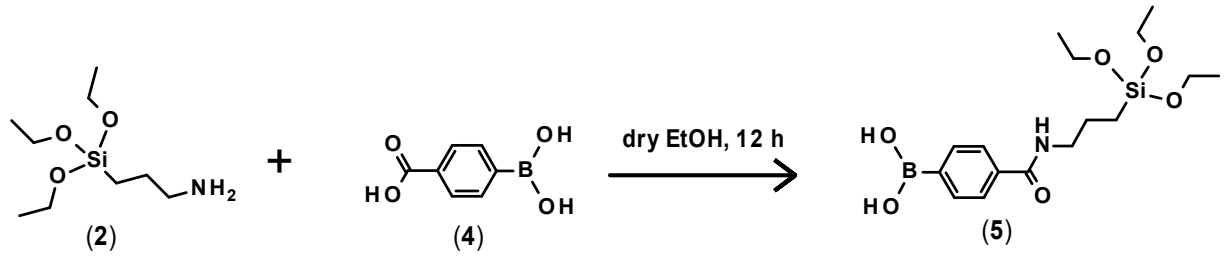

(**2**) (**4**) (**5**)

Scheme S2: Synthesis of triethoxysilanepropyl-3-amido phenylboronic acid (TES-prAmPBA, **5).**

1.3.3 Synthesis of FITC-doped silica nanoparticles (FITC@SiO_2NPs), **Scheme S3**

The fluorescent FITC-doped silica nanoparticles were prepared using a water-in-oil microemulsion method with some modifications.[3] The microemulsion solution was prepared by mixing n-hexanol (3.50 mL), cyclohexane (15.0 mL), Triton X-100 (3.20 mL), and water (1.50 mL). The solvent mixture was stirred for 20 min to form a stable microemulsion. FITC-APTES (**3**, 2.63 mg, 6.75 mol), TEOS (0.60 mL, 2.70 mmol), and NH_4OH (0.060 mL, 1.50 mmol) were added to the microemulsion, and the mixture was stirred at room temperature in the dark for 24 hours. Acetone (30.0 mL) was added to break the microemulsion and isolate the nanoparticles from the solution. Silica nanoparticles were collected by centrifugation and washed with a 1:1 mixture of ethanol/water with repeated sonication and centrifugation (3000 rpm, 5 min, three times) to remove unreacted reagents. The isolated yellow-orange FITC@SiO_2NPs were dried at 40^{o}C overnight in the oven. The FITC-APTES **(3)** dye loadings to the microemulsion were achieved by adding 1.31 mg (3.0%, 3.37 μmol), and 2.63 mg (6.0 %, 6.75 μmol).

FTIR [(ATR), τ_{max}/cm^{-1}]: 3287 (O-H), 1036 (Si-O-Si), 948 (Si-OH), 786 (Si-O). UV-Vis [λ (nm), log (ε)]: 495 (3.8).

1.3.4 Phenylboronic acid functionalization of FITC-doped silica nanoparticles

FITC@SiO_2NPs (20.0 mg) were dispersed in ethanol (5.0 mL) and under stirring for 20 min. TES-PBA (**5,** 40.0 mg, 0.10 mmol) in ammonium solution was added to the nanoparticle ethanol solution. The resulting solution was continuously mixed at room temperature overnight in the dark. The product, phenylboronic acid functionalized-silica nanoparticles (FITC@SiO_2-PBANPs) was obtained after centrifugation as dry products. It was washed several times in a 1:1 mixture of water/ethanol to remove unreacted reagents. The FITC@SiO_2-PBANPs were dried for 48 hours in the dark.

FTIR [(ATR), τ_{max}/cm^{-1}]: 3303 (NH), 1647 (C=O), 1395 (B-O), 1062 (O-Si-O), 949 (Si-O), 785 (Si-OH). UV-Vis [λ (nm) log (ε)]: 495 (3.8).

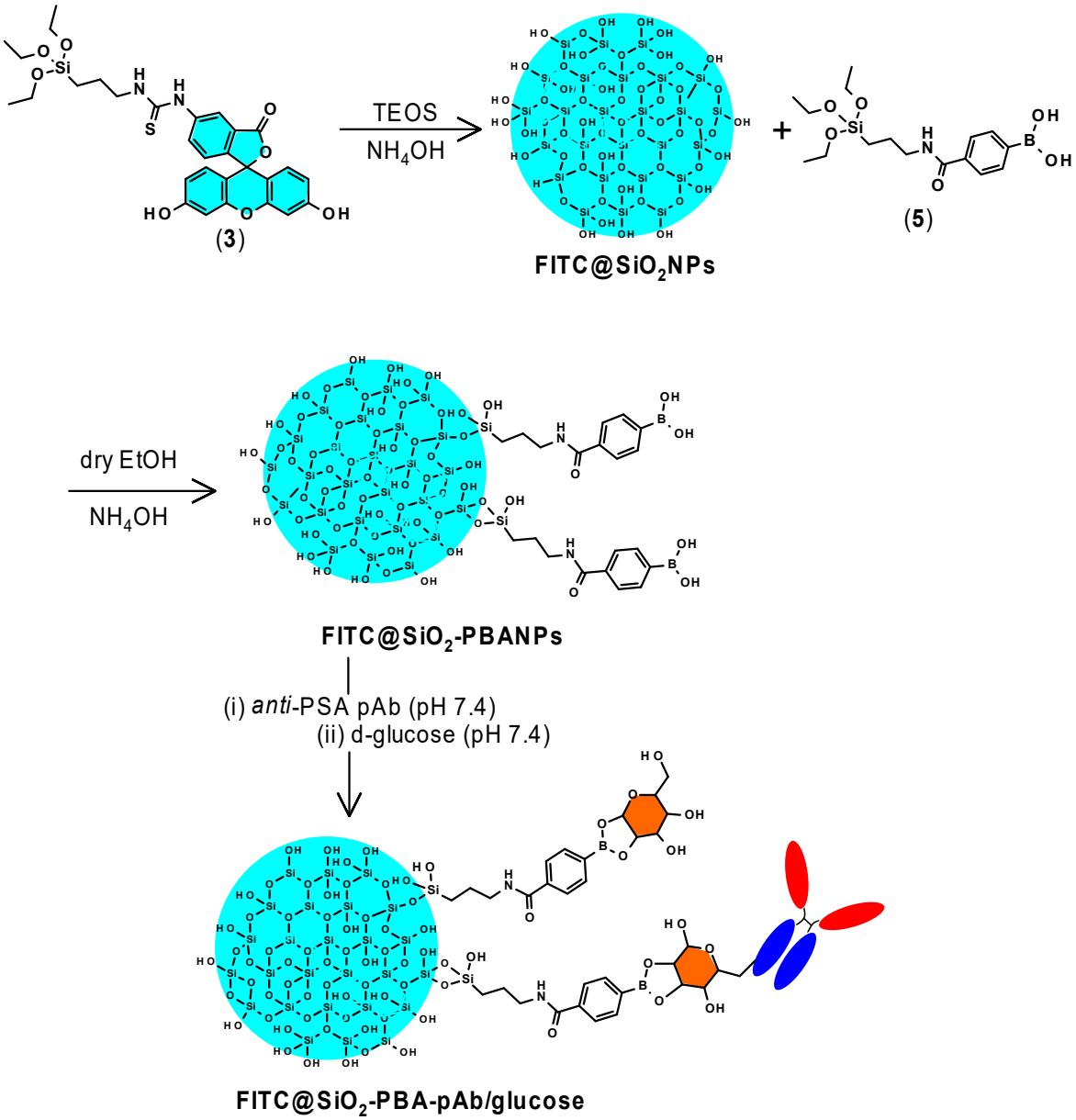

Scheme S3: Preparation of the FITC@SiO_2-PBA-pAb/glucose sensing nanobioconjugates.

1.3.5 Bradford assay for *anti*-PSA pAb onto FITC@SiO_2-PBANPs

The *anti*-PSA polyclonal antibody was covalently attached to the surface of FITC@SiO_2-PBANPs. The bioconjugation of polyclonal *anti*-PSA antibodies onto

FITC@SiO_2-PBANPs was achieved through the boronate ester reaction. The reaction targets the carbohydrate moiety of (N-glycans) on the Fc region of the *anti*-PSA polyclonal antibody. The glycosylation found in the Fc region of the antibody was used to react with the boronic acid functional group of FITC@SiO_2-PBANPs to form cyclic ester bonds. Bradford assay was used as a quantitative colorimetric assay to confirm the immobilization of the *anti*-PSA pAb. The *anti*-PSA pAb in the bioconjugation solution before and after the reaction with the nanoparticles was measured. The FITC@SiO_2-PBA-pAbs after conjugation were centrifuged and the supernatant was used for protein determination. Bovine Serum Albumin (BSA) standard solutions and the supernatant obtained after FITC@SiO_2-PBA-pAbNPs were made to react with Bradford reagent at room temperature for 30 mins. UV-vis spectra were used to follow the bioconjugation of the polyclonal *anti*-PSA antibodies.

1.3.6 Photostability and dye leakage studies

For photobleaching studies, an aqueous solution of FITC (**1**, 1.0 $mg.mL^{-1}$), FITC-APTES (**3**, 1.0 $mg.mL^{-1}$), and FITC@SiO_2NPs (1.0 $mg.mL^{-1}$) were prepared and measured, respectively. The suspensions were radiated under a 300 W xenon lamp and fluorescence spectra recorded at 1 min intervals.

For dye-leaking studies, the FITC@SiO_2NPs suspension (1.0 $mg.mL^{-1}$) was sonicated for 5 min and thereafter centrifuged at 3000 rpm for 5 min. The fluorescence intensity (I_o) of the supernatant was measured. After every 10 min interval, the suspension was sonicated for 5 min, centrifuged at 3000 rpm for 5 min and the fluorescence intensity

of the supernatant solutions (***I***) was measured over time. The amount of the dye retained in the silica matrix was defined as 1-($\frac{I}{I_o}$) as reported.[4,5]

1.3.7 Dye-loading studies of 3.0% and 6.0% w/w

A dye-loading test was to estimate the number of FITC molecules encapsulated per fluorescent silica nanoparticle. In the dye-loading experiment, an aqueous suspension of FITC@SiO_2NPs (1.0 mg.mL^{-1}) was sonicated for 10 min and incubated for 1 hour at 37^{o}C. Then, the ground state absorption and fluorescence emission spectra of the solution measured before and after dissolution with NaOH (1.0 mL, 10 mM). The absorption intensities and TEM sizes of the silica nanoparticles were used to estimate the numbers of FITC molecules loaded per nanoparticle for each altered loading and were calculated as reported.[6]

1.3.8 Fluorescence Quantum Efficiency

The fluorescence quantum efficiency studies of the as-prepared 3.0 and 6.0 (%, w/w) FITC@SiO_2NPs against the standard FITC dye were monitored using fluorescence measurements. A standard solution of FITC (**1**, 1.0 mg.mL^{-1}) and an aqueous solution of FITC@SiO_2NPs (1.0 mg.mL^{-1}) at 3.0 and 6.0 (%, w/w) dye loadings were prepared and sonicated for 10 min. The absorption and fluorescence intensity (I_o) of the suspensions measured. After a solution of NaOH (1.0 mL, 0.010 M) was added to the 3.0 and 6.0 % (w/w) FITC@SiO_2NPs suspensions, the reaction was allowed to react

for 30 min. The dissolution of FITC@SiO_2NPs occurred and released FITC molecules. The experiment followed the FITC **(1)** and FITC@SiO_2NPs after dissolution. We observed a linear calibration curve of the integrated fluorescence intensity (emission peak area) as a function of solution absorbance and further obtained the quantum yield measurements using the gradients determined using **Eq. (1)**.

$$\% \, \Phi_{NPs} = 100 \, (\Phi_{Fstd} \, x \, \frac{m_{NPs}}{m_{Fstd}} \, x \, \frac{\eta^2_{NPs}}{\eta^2_{Fstd}}) \qquad \textbf{(1)}$$

where Φ_{NPS} is the quantum yield of the nanoparticles, m_{NPS} and m_{std} integrated fluorescence intensity slopes of the FITC@SiO_2NPs and the fluorescein standard Φ_{Fstd} (= 0.97), respectively. η_{NPS} and η_{Fstd} are the refractive indexes of the medium.[7]

2 Results and Discussion

2.1 FTIR Spectra of FITC-APTES (3)

Figure S1(i) shows the FTIR spectrum of FITC **(1)** with the characteristic isothiocyanate (N=C=S) stretching peak at 2027 cm^{-1}, the aromatic CH (Φ-CH) stretching peaks at 2971 cm^{-1}, and the vibrational peaks due to the xanthene ring (C=C) stretch at 1545 cm^{-1}, 1536 cm^{-1}, and 1458 cm^{-1}. Lastly, the carbonyl group (C=O) of lactone (Φ-O-C=O) vibrational peak is exhibited at 1619 cm^{-1}, a (C-O-C) group at 1052 cm^{-1} and O-H peaks at 3677 cm^{-1}**. Figure S1(ii)**, the FT-IR spectrum of APTES **(2)** shows the characteristics of siloxane (O-Si-C) vibrational bands at 1019 cm^{-1}, (O-Si-O) stretching vibrations at 1103 cm^{-1}, and (Si-O) stretching vibration at 949 cm^{-1}. Additionally, the N-H asymmetric and symmetric stretching peaks of the propylamine group of APTES **(2)** were found at 3289 cm^{-1} and 3350 cm^{-1}, along with the bending vibrations at 1603 cm^{-1}. Lastly, aliphatic (CH) peaks were found at 2926

cm^{-1} and 2928 cm^{-1}, respectively. The formation of FITC-APTES **(3)** conjugate was monitored by the disappearance of the isothiocyanate (N=C=S) stretching vibrations of FITC **(1)**. **Figure S1(iii)** shows the FT-IR spectrum of FITC-APTES **(3)** with the characteristic peaks corresponding to both the FITC **(1)** and APTES **(2)**. The disappearance of the isothiocyanate (N=C=S) at 2027 cm^{-1} was observed. The formation of the thiourea bond, -N-C(=S)-N at 1309 cm^{-1} confirmed the successful synthesis of FITC-APTES (**3**). [1,2] The band at 1570 cm^{-1} was due to the thioamide (N-C=S) vibrations.[8] The bands at 3359 cm^{-1} were due to N-H stretching vibrations of the thiourea group. Lastly, the (O-Si-O) stretching was at 1103 cm^{-1}, and (Si-C) bending vibrations was at 949 cm^{-1}. The aliphatic (CH) peaks are observed at 2869 cm^{-1} and 2930 cm^{-1} from APTES moiety.

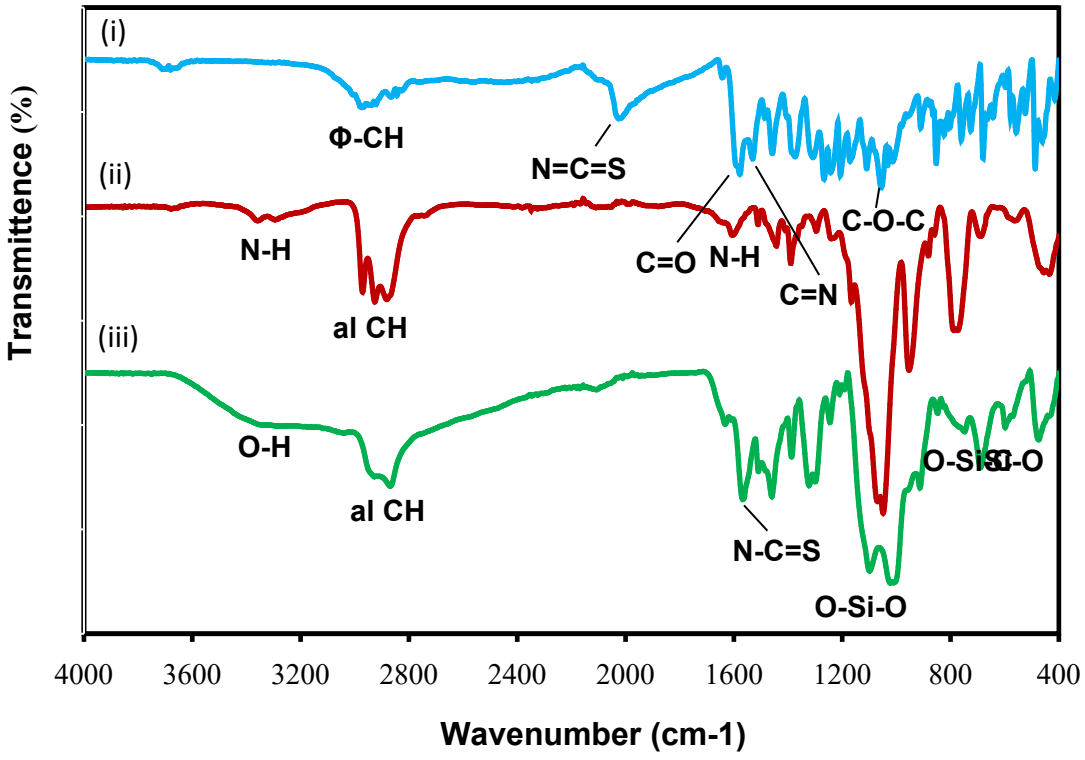

Figure S1: FT-IR spectra of (i) Fluorescein-5-isothiocyanate (FITC, **1**), (ii) (3-amino

propyl)triethoxysilane (APTES, **2**), and (iii) fluorescein-isothiocyanito-3-propyl triethoxysilane (FITC-APTES, **3**).

2.2 FTIR characterization of triethoxysilanepropyl-3-amido phenylboronic acid, TES-BPA (**5**)

Figure S2(i) the FT-IR spectrum of 4-CPBA **(4)** shows the (O-H) stretch of the boronic acid at 3342 cm^{-1}, aromatic C-H (Φ-CH) stretching peak at 3124 cm^{-1}, and an intense (C=O) from the carboxylic acid (COOH) peak at 1680 cm^{-1}. The B-O vibrational stretches were observed at 1321 cm^{-1} and 849 cm^{-1}. The FTIR spectrum of APTES in **Fig. S2(ii)** is the same as in **Fig. S1(ii)** and as discussed above. **Figure S2(iii)** shows the spectrum of the TES-PBA **(5)** and the disappearance of the primary amine (NH_2) from APTES **(2)** at 1575 cm^{-1} in **Figure S2(ii)**, and the appearance of the carbonyl (C=O) stretch for an amide bond (N-C=O) at 1639 cm^{-1}. The carbonyl (C=O) has shifted from 1680 cm^{-1} for 4-CPBA (**4**) to 1638 cm^{-1}. Also, the O-H stretch of the boronic acid was retained at 3526 cm^{-1} and shifted from 3342 cm^{-1} of 4-CPBA **(4)**. The secondary amide stretch (N-H) at 3316 cm^{-1} is observed. This indicated the presence of the amide bond formation between APTES **(2)** and 4-CPBA **(4)**. The C-H stretches due to aromatic (Φ-CH) and aliphatic (al-CH) were observed at 3226 cm^{-1} and 2955 cm^{-1}, respectively. The B-O stretch was observed at 1317 cm^{-1}, and this slightly shifted in TES-PBA **(5)** when compared to 4-CPBA **(4)**. The presence of the characteristic peak at 1060 cm^{-1} was attributed to the O-Si-O from the APTES **(2)** moiety. The observed changes confirm the successful synthesis of triethoxysilanepropyl-3-amido phenylboronic acid, TES-PBA (**5**).

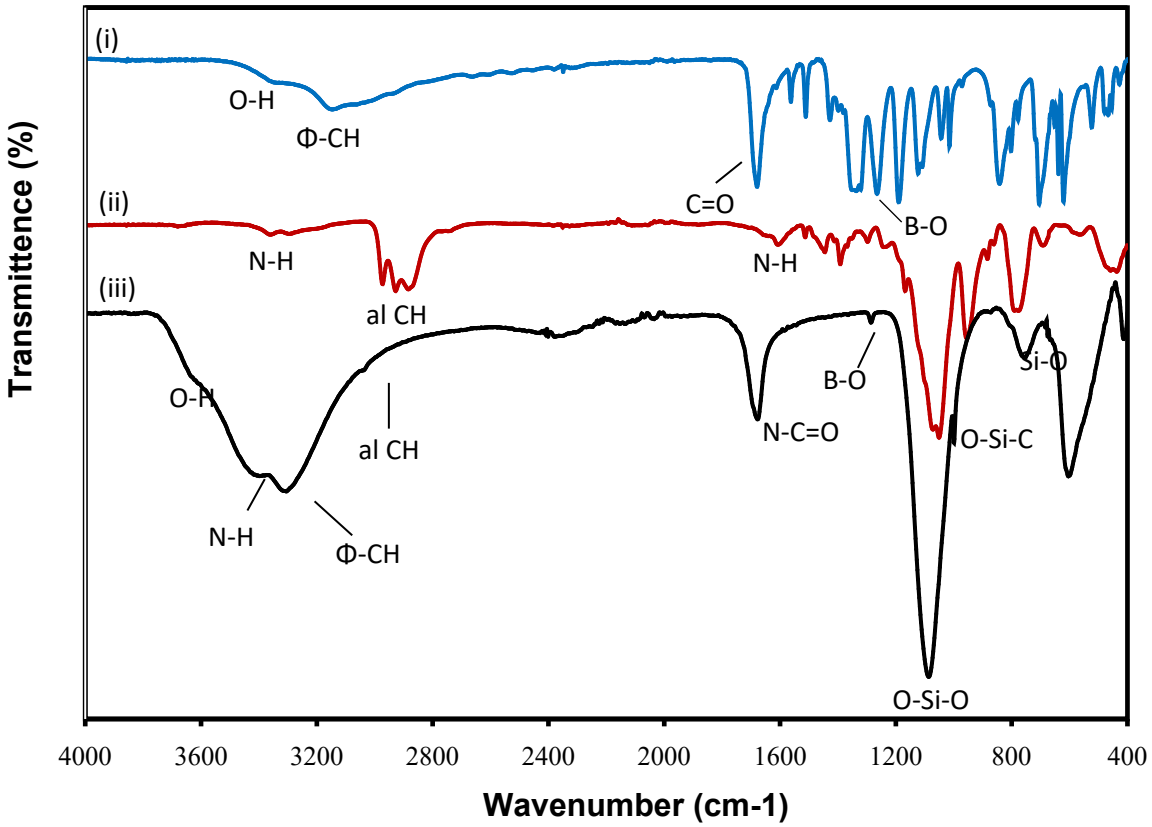

Figure S2: FTIR spectra of (i) 4-carboxyphenylboronic acid, 4-CPBA (**4**), (ii) APTES **(2)**, and triethoxysilanepropyl-3-amido phenylboronic acid, TES-PBA (**5**).

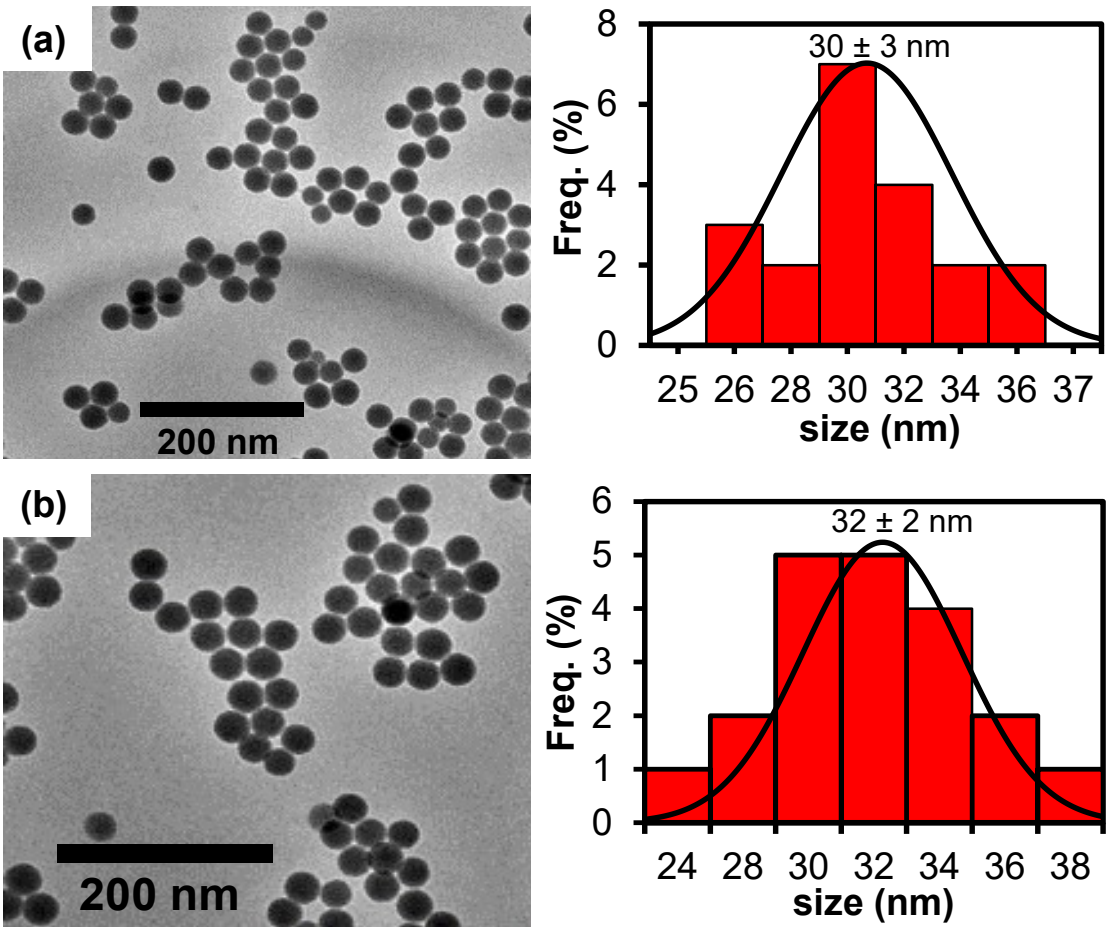

Figure S3: TEM micrographs and corresponding histograms of 3% (a) FITC@SiO_2NPs, and (b) FITC@SiO_2-PBANPs

2.3 Energy Dispersive X-ray Spectroscopy (EDS)

The encapsulation of FITC-APTES **(3)** and modification of FITC@SiO_2NPs with TES-PBA **(5)** and *anti*-PSA pAb were confirmed by EDS. **Figure S4** shows the EDS spectra of FITC-APTES **(3)**, (b) FITC@SiO_2NPs, (c) FITC@SiO_2-PBANPs and FITC@SiO_2-PBA-pAb/glucose. From **Figure S4(a)**, the silica peak (Si K) from FITC-APTES **(3)** was observed. The sulfur (S K), oxygen (O K), nitrogen (N K), and carbon (C K) are from the FITC after the successful synthesis of conjugate FITC-APTES **(3)**. The elemental composition confirmed the FITC-APTES (**3**) compound, especially the S K (1.6%) and N K (3.7%) ration of 1:2 as per the chemical structure. **Figure S6(b)** shows

an increase in the silica (Si K) and oxygen (O K) peaks after the encapsulation of FITC-APTES **(3)** with tetraethylorthosilicate (TEOS) to form FITC@SiO_2NPs. TEOS introduces additional Si K and O K during the formation of the nanoparticles (FITC@SiO_2NPS). The increase in the elemental composition for Si K from 11.9% to 39.1% and for O K from 30.6% to 50.6% confirm the successful synthesis. **Figure S6(c)** shows the presence of the boron peak (B K, 15.7%) attributed to the phenylboronic acid, which reveals the successful formation of FITC@SiO_2-PBANPs. An increase in the C K elemental composition from 7.8% to 15.5% confirmed the functionalization of TES-PBA (**5**) onto the FITC@SiO_2NPs to form FITC@SiO_2-prAmPBANPs. After bioconjugation of *anti*-PSA pAb in **Figure S6(d)**, the O K and N K elemental composition increased confirming the antibody attachment. The bioconjugated nanoparticle was represented as FITC@SiO_2-PBA-pAb/glucose. The O K elemental composition increased from 45.7% to 47.3% and for N K was from 0% to 4.3% due to the protein (*anti*-PSA pAb). The presence of the silica peak in all materials was an indication that the silica nanomaterial stayed intact during the various functionalization steps.

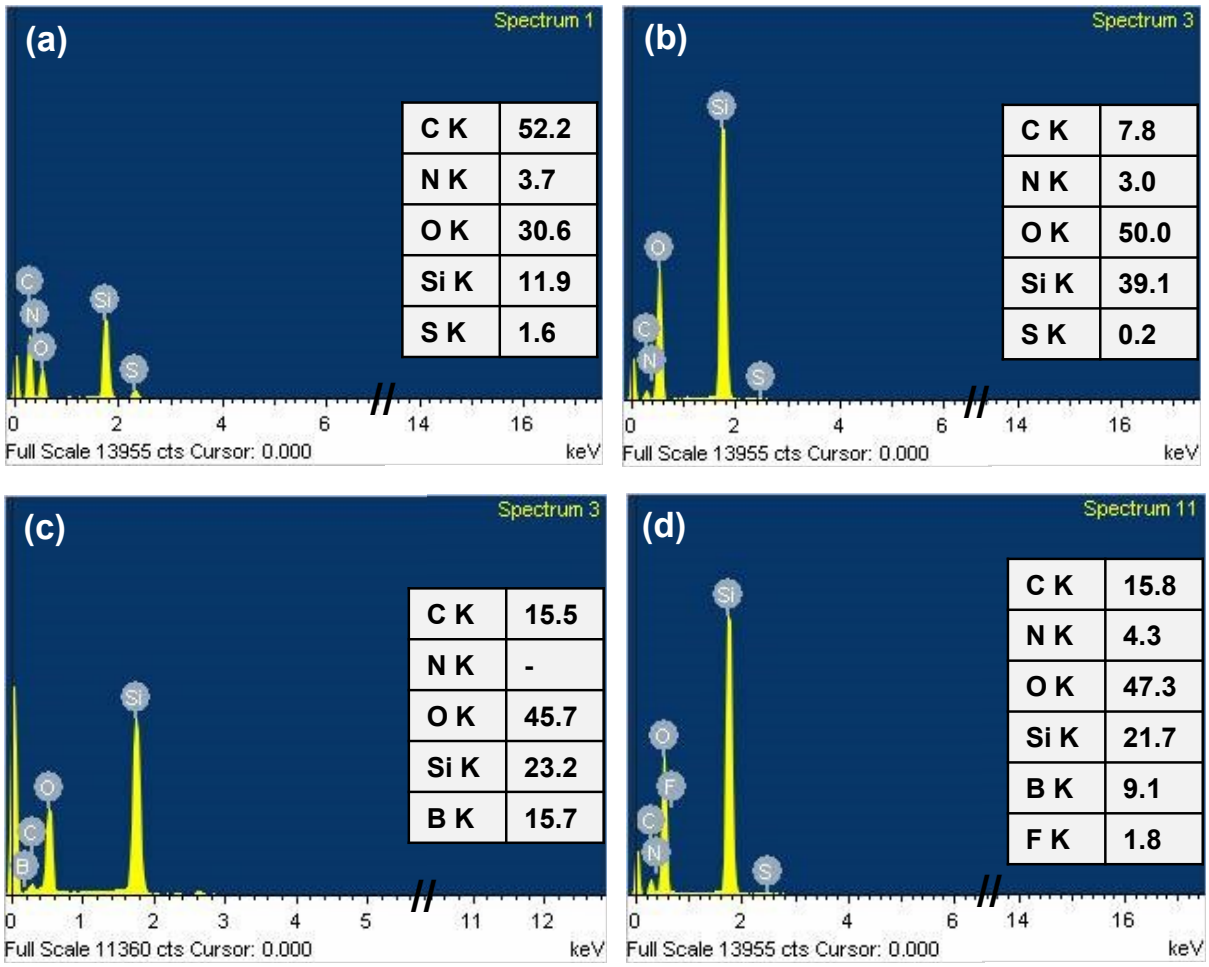

Figure S6: The EDS images and corresponding elemental composition of (a) FITC-APTES (**3**), and 6% (b) FITC@SiO_2NPs, (c) FITC@SiO_2-PBANPs, and (d) FITC@SiO_2-PBA-pAb/glucose.

2.4 Dye-loading and Fluorescence Quantum Efficiency Studies

The dye-loading experiment was carried out to determine the possible occurrence of the HOMO-FRET (highest occupied molecular orbital-fluorescence resonance energy transfer) upon loading of FITC-APTES **(3)** into the silica nanoparticles. The study observed the optimization of the altered dye-loaded fluorescent silica nanoparticles for high sensitivity and signal amplification studies. **Figure S7(a)** shows the ground-state absorption and fluorescence emission spectra of the 3.0% and 6.0%, w/w dye-loaded FITC@SiO_2NPs. The absorption intensity increases with an increase in the %, w/w of

FITC-APTES **(3)** loaded. The increase in the intensity is related to the number of FITC-APTES **(3)** molecules incorporated within the FITC@SiO_2NPs. An increase in %, w/w indicated that more FITC-APTES **(3)** molecules were loaded into the 6.0% FITC@SiO_2NPs. Furthermore, the number of FITC-APTES **(3)** molecules per FITC@SiO_2NPs was estimated to be 6.02 x 10^{26} for 3.0% and 3.23 x 10^{28} for 6.0% w/w loadings, as shown in **Table S1**. The fluorescence emission intensity also increased with increasing %, w/w FITC-APTES **(3)** loading in nanoparticles from 3.0% to 6.0%. The 6.0 (%, w/w) exhibited a higher fluorescence intensity as compared with the 3.0 (%, w/w) FITC@SiO_2NPs. Both silica nanoparticles exhibited negligible quenching, indicating a reduced dye-dye intermolecular interaction. The fluorescence quantum efficiency for both the 3.0% and 6.0% (w/w) FITC@SiO_2NPs was measured to determine the fluorescence efficiency of the FITC-APTES **(3)** before and after dissolution. **Figure S7(b)** shows the fluorescence quantum efficiency of FITC@SiO_2NPs (before and after dissolution) against FITC **(1)**. From **Figure S7(b)**, the fluorescence quantum efficiency of FITC@SiO_2NPs increased with increasing %, w/w FITC-APTES **(3)** loading. The standard FITC **(1)** was used as a 100% quantum efficiency. The fluorescence efficiency of 3.0% w/w FITC@SiO_2NPs was 57% and 77% for the 6.0% w/w. The fluorescence efficiency of both silica nanoparticles was lower than that of FITC **(1)** before the addition of NaOH solution (10 mM). The results showed that at a higher % w/w, loading, higher fluorescent emission is expected due to increased FITC-APTES **(3)** molecules in the silica nanoparticles. The quantum efficiency results corresponded to the trend observed for fluorescence emission intensity in **Figure S7(a)**. The quantum efficiency of the FITC@SiO_2NPs with different FITC-APTES **(3)** loading after dissolution with NaOH increased. The NaOH leads to the breaking up of the silica nanoparticles and dissolution of the silica shell for

FITC@SiO_2NPs releasing the FITC-APTES **(3)** molecules into solution. The FITC-APTES **(3)** molecules in solution fluorescence without interference. The result as shown in **Figure S7(b)**, the 6.0% FITC@SiO_2NPs exhibited an increase in its fluorescence quantum efficiency from 77% to 96% as compared to the 3.0% FITC@SiO_2NPs loading. The quantum efficiency of the 6.0% FITC@SiO_2NPs was close to 100% as compared to the efficient quantum efficiency of FITC **(1)**. Therefore, the 6.0% FITC@SiO_2NPs with a uniform monodispersed morphology shown in the TEM images in **Figure 2**, and an efficient fluorescence quantum efficiency (96%) after dissolution with NaOH solution was favourable as sensing nanobioconjugates for PSA detection.

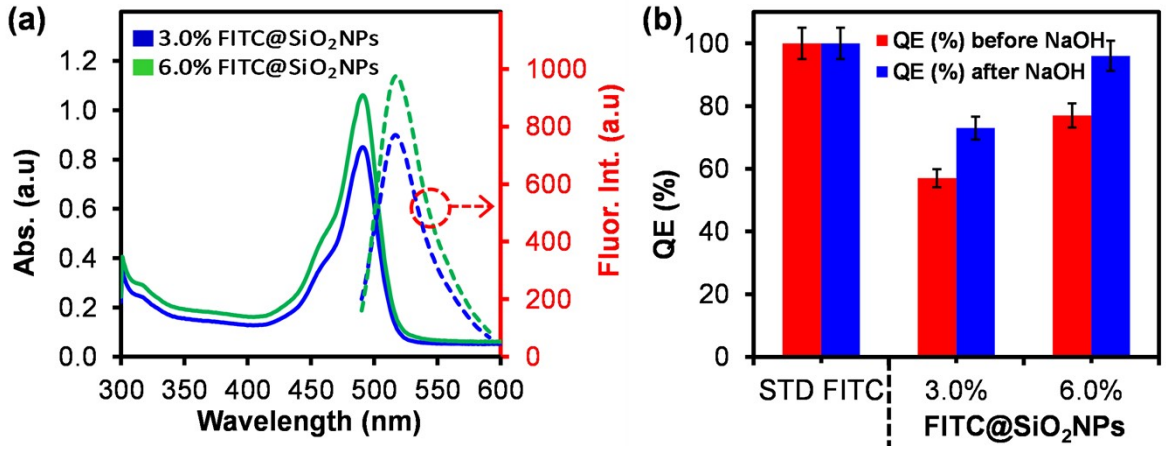

Figure S7: (a) Ground-state absorption and fluorescence emission spectra, and (b) the fluorescence quantum efficiency of FITC@SiO_2NPs before and after the addition of NaOH (10 mM). All samples were diluted in 10 mM PBS buffer pH (7.4) (n =3).

2.5 Bradford Assay pAb onto FITC@SiO_2-PBANPs

The Bradford assay was used to determine the amount of *anti*-PSA polyclonal antibodies (pAbs) conjugated onto FITC@SiO_2-PBANPs. UV-vis measurements were obtained at 595 nm which corresponded to the BSA standard solutions and protein (pAb) in solution. The calibration curve of known BSA concentrations is shown in **Figure S8(b)** was used to extrapolate and determine the concentrations of the pAb in the supernatant solution. The absorbance of the used volumes of the BSA standard solutions and protein suspension were recorded in triplicates. Therefore, mean values were determined and found to range from 0.25 ± 0.090 to 0.34 ± 0.090 a.u with very low standard deviations. The mean value of the unknown concentration of the pAbs suspension was 0.27 ± 0.02 a.u and recorded as a representative value of the absorbance of pAbs. Then, this value was fitted into the calibration curve, along with the BSA standard solutions, and used to calculate the concentration of the pAbs after bioconjugation. The slope (ΔAbs = 0.0033 [BSA] + 0.2557) was used to determine the concentration of the unknown pAbs and was found to be 8.70 µg.mL^{-1}.

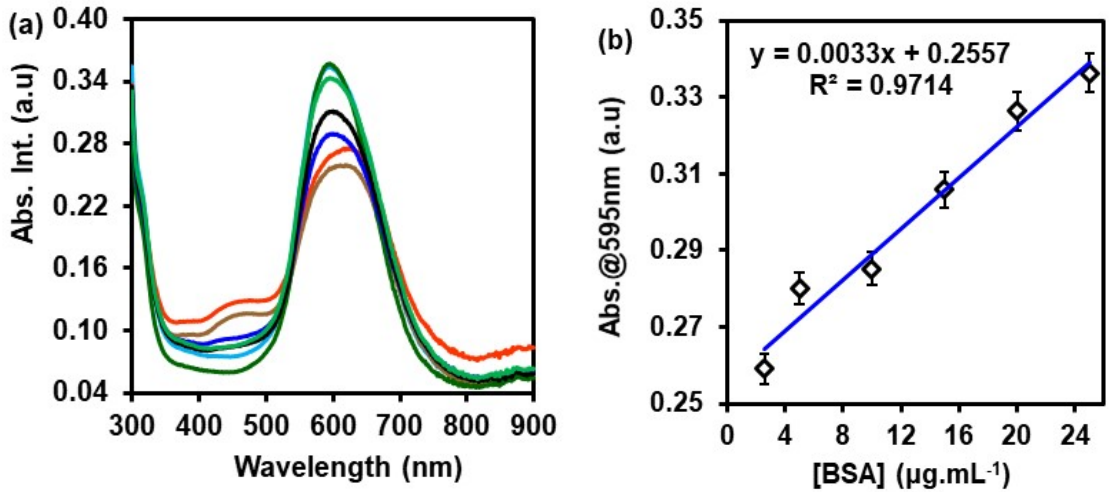

Figure S8: (a) UV-Vis spectra of different BSA standards and pAbs concentrations, (b) the corresponding calibration curve (n = 3).

2.6 Dye-leakage and photostability study

The photostability study of (a) FITC **(1)**, (b) FITC-APTES **(3)**, and (c) FITC@SiO_2NPs over 50 min was investigated and **Fig. S9** shows the changes in intensity over time. The amount of dye encapsulated in FITC@SiO_2NPs was also studied. The excitation wavelength values used was 480 nm. The emission values were obtained at 520 nm FITC **(1)**, 518 nm for both FITC-APTES **(3)**, and FITC@SiO_2NPs. **Fig. 4(b)** and the discussion on section 3.4.2 in the manuscript shows the analysed data and interpretation.

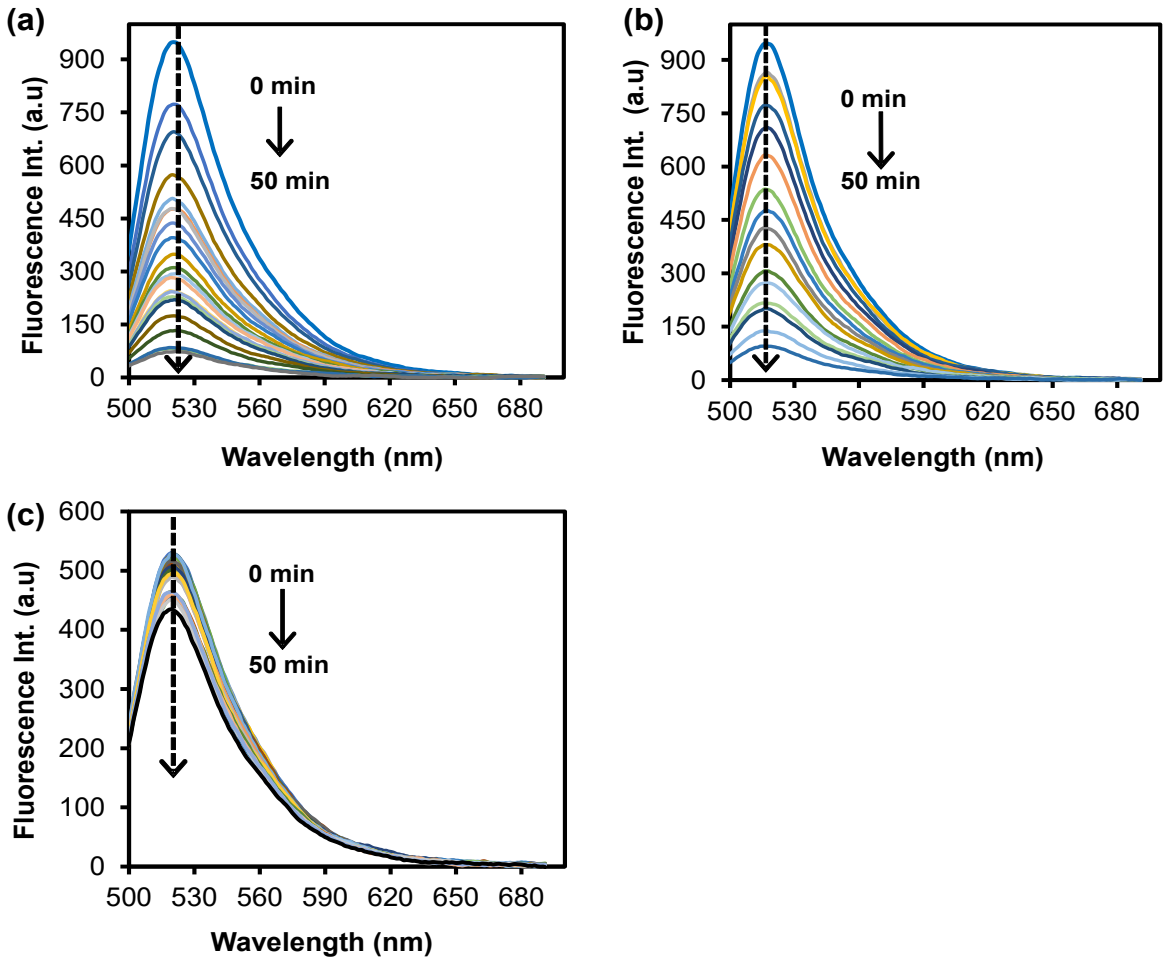

Figure S7: Fluorescence spectra of (a) FITC **(1)**, (b) FITC-APTES **(3)**, and (c) FITC@SiO_2NPs. All samples were diluted in PBS buffer 7.4 and measurements were taken at 5-min intervals.

2.7 FITC-APTES (**3**) loading ratio

The number of FITC-APTES **(3)** molecules encapsulated per FITC@SiO_2NPs was estimated from absorption readings. The estimations were investigated by dissolving an equal amount of the FITC@SiO_2NPs of (3.0% and 6.0%,w/w) dye loadings with NaOH (10 mM).[9] The absorption intensity reading of the dissolved FITC@SiO_2NPs was recorded. The adsorption intensity was used to calculate the number of FITC-APTES **(3)** molecules per silica nanoparticles using a molar extinction coefficient (∑) of FITC **(1)** and the TEM size. From the TEM size (diameter, d), the average volume of a single FITC@SiO_2NP was obtained using **Eq. (1):**

$$V_{FITC@SiO2NP} = \frac{4}{3}\pi\left(\frac{d}{2}\right)^3 \quad \textbf{(1)}$$

The total number of FITC@SiO_2NP in the suspension was calculated based on the dry weight and the density of the amorphous silica matrix (2.22 g.cm^{-3}).[10] The total number of FITC-APTES **(3)** (FITC-APTES$_{tot}$) from the dissolved nanoparticles was determined from the absorption intensity after the dissolution using **Eq. (2)**:

$$FITC - APTES_{tot} = \frac{(6.022\ x\ 10^{23})(A)}{\varepsilon l} \quad \textbf{(2)}$$

where *l* is the path length (1 cm), A is the absorption intensity, and *ε* is the molar absorptivity of FITC (73,000 cm^{-1}.M^{-1}). The number of FITC-APTES **(3)** molecules per FITC@SiO_2NP is equal to FITC-APTES **(3)** per unit volume divided by the number of FITC@SiO_2NP per unit volume as expressed in **Eq. (3):**

$$n_{FITC-APTES} = \frac{FITC - APTES_{tot}}{n_{FITC@SiNP}} \quad \textbf{(3)}$$

Where $n_{FITC\text{-}APTES}$ is the number of FITC-APTES **(3)** molecules per FITC@SiO_2NP, $FITC\text{-}APTES_{tot}$ is the total number of FITC-APTES **(3)** molecules and $n_{FITC@SiO2NPs}$ is the number of FITC@SiO_2NP in suspension. The total number of FITC@SiO_2NPs in suspension, the average volume of the as-synthesized FITC@SiO_2NP, and the number of FITC-APTES **(3)** per FITC@SiO_2NP at 3.0 % and 6.0 % FITC-APTES **(3)** loading are summarised in **Table S1**. The average volume of the FITC@SiO_2NP increased with an increase in TEM size. The number of FITC molecules per FITC@SiO_2NP also increased from 3.0 % to 6.0 % loading, confirming that with an increase in FITC molecules doped into the silica nanoparticles.

Table S1: Determination of the number of FITC-APTES **(3)** molecules loaded per fluorescent silica nanoparticle using TEM and UV-absorption values.

% w/w	TEM Size (nm)	Average Volume (cm^3)	Nanoparticles in suspension (particles)	FITC-APTES **(3)** molecules in suspension (moles)	FITC-APTES **(3)** per nanoparticle (moles)
3.0	30	1.56×10^{-17}	7.05×10^{15}	7.15×10^{18}	6.07×10^{26}
6.0	46	5.79×10^{-17}	1.89×10^{15}	1.02×10^{19}	3.23×10^{27}

3. References

1 L. Friedrichs, A simple cleaning and fluorescent staining protocol for recent and fossil diatom frustules, *Diatom Res.*, 2013, **28**, 317–327.

2 E. Gök and S. Olgaz, Binding of Fluorescein Isothiocyanate to Insulin: A Fluorimetric Labeling Study, *J. Fluoresc.*, 2004, **14**, 203–206.

3 O. K. Adeniyi, A. Ngqinambi and P. N. Mashazi, Ultrasensitive detection of anti-p53 autoantibodies based on nanomagnetic capture and separation with fluorescent sensing nanobioprobe for signal amplification, *Biosens. Bioelectron.*, 2020, **170**, 112640.

4 P. D. K. P. Ananda, A. Tillekaratne, C. Hettiarachchi and N. Lalichchandran, Sensitive detection of E. coli using bioconjugated fluorescent silica nanoparticles, *Appl. Surf. Sci. Adv.*, 2021, **6**, 100159.

5 L. Min, L. Zhao-Yue, L. Qiang, Y. Hang, M. Lan, L. Jing-Hong, B. Yu-Bai and L. Tie-Jin, Functionalized Fluorescein-doped SiO2 Nanoparticles for Immunochromatographic Assay, *Chinese J. Chem.*, 2005, **23**, 875–880.

6 C. J. Moore, G. Giovannini, F. Kunc, A. J. Hall and V. Gubala, 'Overloading' fluorescent silica nanoparticles with dyes to improve biosensor performance, *J. Mater. Chem. B*, 2017, **5**, 5564–5572.

7 X. Zhao, R. P. Bagwe and W. Tan, Development of Organic-Dye-Doped Silica Nanoparticles in a Reverse Microemulsion, *Adv. Mater.*, 2004, **16**, 173–176.

8 I. Suzuki, Infrared Spectra and Normal Vibrations of Thioamides. III. N -Methylthioformamide and N -Methylthioacetamide, *Bull. Chem. Soc. Jpn.*, 1962, **35**, 1456–1464.

9 C. L. O'Connell, R. Nooney and C. McDonagh, Cyanine5-doped silica nanoparticles as ultra-bright immunospecific labels for model circulating tumour cells in flow cytometry and microscopy, *Biosens. Bioelectron.*, 2017, **91**, 190–198.

10 V.M. Masalov, N.S. Sukhinina, E.A. Kudrenko, G.A. Emelchenko, Mechanism of formation and nanostructure of Stober silica nanoparticles, *Nanotechnology* 2011, **22**, 275718.